

## Adsorption Characteristics of Coconut Husk Biochar for Organics in Water

Vo Cong Minh<sup>1,2,3</sup>, Nguyen Nhat Huy<sup>2,3</sup>, Thuy Nguyen Thi<sup>3,4</sup>, and Lien Thi Le Nguyen<sup>3,5\*</sup>

<sup>1</sup>Faculty of Chemistry, Ho Chi Minh City University of Education (HCMUE), 280 An Duong Vuong Street, District 5, Ho Chi Minh City 700000, Vietnam

<sup>2</sup>Faculty of Environment and Natural Resources, Ho Chi Minh City University of Technology (HCMUT), 268 Ly Thuong Kiet Street, District 10, Ho Chi Minh City 700000, Vietnam

<sup>3</sup>Vietnam National University Ho Chi Minh City (VNU-HCM), Linh Trung Ward, Thu Duc District, Ho Chi Minh City 700000, Vietnam

<sup>4</sup>School of Chemical and Environmental Engineering, International University (HCMIU), Quarter 6, Linh Trung Ward, Thu Duc City, Ho Chi Minh City 700000, Vietnam

<sup>5</sup>Faculty of Chemical Engineering, Ho Chi Minh City University of Technology (HCMUT), 268 Ly Thuong Kiet Street, District 10, Ho Chi Minh City 700000, Vietnam

**\* Corresponding author:**

tel: +84-932640912

email: ntlilien@hcmut.edu.vn

Received: September 5, 2024

Accepted: January 27, 2025

DOI: 10.22146/ijc.99722

**Abstract:** Biochar was produced from coconut husk by simple pyrolysis at 600 °C, aiming for low-cost production. The biochar was characterized and studied for adsorption of four types of antibiotics and organic contaminants, which were levofloxacin (LEV), doxycycline (DOX), tartrazine (Tar), and rhodamine B (RhB), in water. The EDX and FTIR analysis shows homogeneous active centers of the biochar. The high surface area, i.e., 664.66 m<sup>2</sup>/g, and total pore volume of 0.8159 cm<sup>3</sup>/g were determined by BET analysis, and the pore structure observed in SEM shows the appropriation of the material for adsorption of organic contaminants in the water. Adsorption conditions were studied and the results revealed that the adsorption mechanism varies among different adsorbate's molecular structures. The result shows that cationic dye (RhB) is better absorbed by the coconut biochar than anionic dye (Tar) and the covalent antibiotic (DOX, LEV). The maximal adsorption capacities under optimal pH conditions were 172.41 mgRhB/g, 48.31 mgDOX/g, 42.37 mgLEV/g, and 21.37 mgTar/g. The best experimental fit for the adsorption data was Langmuir isotherm. The thermodynamic studies implied that the adsorption mechanism was physical adsorption (e.g., LEV, DOX, Tar), while RhB adsorption is more likely to be chemisorbed.

**Keywords:** biochar; adsorption; dye; antibiotics; organic contaminants

### ■ INTRODUCTION

The wastewater of industrial and human activities, including dye, humid substances, phenolic compounds, petroleum, surfactants, pesticides, and pharmaceuticals released into aquatic environments, are almost hydrophobic or persistent organic pollutants (POPs), which are resistant to chemical and biological degradation. Organic contaminants pose various risks to human health and the environment. They could exert hepatic, reproductive, developmental, behavioral,

neurologic, endocrine, cardiovascular, and immunologic adverse health effects, disrupt ecosystems, and harm wildlife [1].

Antibiotics are substances extracted from microorganisms or fungi using synthetic or semi-synthetic methods that can kill or inhibit certain types of bacteria. Most antibiotics undergo only partial metabolism by the intended organism. Therefore, 30 to 90% of the antibiotic residues are excreted in urine and feces and eventually end up in the environment or

wastewater treatment plants [2]. After being released into the environment, they can kill beneficial microorganisms or create resistant bacteria. Antibiotics may cause genetic changes through different pathways involving an increase of free radicals inside the cell or oxidative stress by inducing error-prone polymerases mediated by SOS response, misbalancing nucleotide metabolism, or acting directly on DNA [3]. An investigation showed sources and ecological risks related to antibiotics in surface water in the East and Southeast Asian samples from 2007 to 2020 with the result of concentration at 10–100 mg/L on average [4]. Adsorption and biotic degradation were a method for antibiotic removal, with adsorption being a major mechanism for removing tetracyclines, fluoroquinolones, and macolide [5]. RhB is the most toxic among the xanthene dyes and has been widely used in the industry due to its good water solubility, incredible brightness, and good stability. Although RhB dyes are useful due to their desirable properties, they are neurotoxic and carcinogenic, harm the development of organisms, and are generally toxic to the environment. RhB is persistent and cannot be degraded in the light except when the photocatalyst has been added [6]. Tartrazine is a synthetic azo dye used as a food colorant to achieve yellow or green shades in sweets, jellies, juices, jams, mustard, sodas, and pharmaceuticals, such as vitamin capsules, antacids, and cosmetics. Tar is one of the largest effluent contaminants in the food industry. Since its molecular structure contains aromatic rings on both sides of its azo group, it is difficult to degrade [7].

Some methods to remove antibiotics and colorants from wastewater have been widely applied, including chemical flocculation, adsorption, membrane separation, oxidation processes, and biodegradation, among which the adsorption method is effective, simple, and compact but is relatively high cost due to the cost of adsorbent replacement. The adsorption method is widely preferred due to its simplicity and several advantages compared to other removal methods, such as low cost, ease of operation, a wide variety of readily available adsorbents, and minimal sludge generation [2]. A critical factor in the adsorption application is the choice of an adsorbent, which should be cost-effective and easily manufactured.

Biochar has gained attention due to its distinct physicochemical characteristics as amorphous carbon with a high surface area, rich functional groups, cost-effective and efficient adsorbent [8]. Biochar is manufactured from biomass by pyrolysis, which is a process that involves heating organic matter in the total or partial absence of oxygen. Biochar is characterized by its high carbon content, porous structure with high surface area and negative charge, in which properly treated heavy metal and organic contaminants are to be studied [9-11]. Indeed, biochar characteristics are different by feedstocks and pyrolysis techniques in manufacture, which would affect both the physicochemical and structure of the surface [12]. Electrostatic attraction, hydrogen bonding, electron acceptor  $\pi$ - $\pi$  interaction, and hydrophobic interaction were considered to be the forces that result in the organic adsorption [13]. Mechanisms of antibiotic adsorption onto biochar's surface are pH effectiveness, functional groups (electrostatic interaction or electron acceptor or hydrogen bond), and porous structure, and these factors are total [14]. The biochar produced at higher temperatures (i.e., 700 °C) had the adsorption capacity with organics (e.g., doxycycline and ciprofloxacin) higher than the lower temperatures of pyrolysis (i.e., 300–500 °C) [15].

Coconut husk is an extremely available material in Vietnam. This is a popular agricultural waste, especially in the Mekong Delta. Using this material to make biochar will be a convenient and economical application in soil nutrients and wastewater treatment. In this paper, biochar was manufactured from coconut husk by pyrolysis at high temperature (i.e., 600 °C) aiming to adsorb organic pollutants, including antibiotics (i.e., levofloxacin, doxycycline), anionic dyes (i.e., tartrazine), and cationic dyes (i.e., RhB). The adsorption ability was compared by molecular structure particularly, and the adsorption mechanism of the system was investigated.

## ■ EXPERIMENTAL SECTION

### Materials

The coconut husk was collected in Dong Thap province, Vietnam. The chemicals were produced by the Xinyang Chemical Reagent factory (China). The water

used in the study was double-distilled.

### Instrumentation

The biochar's porous structure was examined by Brunauer-Emmett-Teller (BET) analysis using a surface analyzer (Thermo Scientific, USA). The crystalline structure of the biochar was studied by X-ray diffraction (XRD) using the D2 Phaser system (Bruker, Germany). The morphology of biochar was observed by scanning electron microscopy (SEM) using JSM-IT200 machine (JEOL, Japan), plus the percentage and distribution of elements in the biochar was illustrated by energy-dispersive X-ray spectroscopy (EDX) using a JSM-IT machine (JEOL, Japan). The biochar's surface chemical properties were analyzed by Fourier-transform infrared spectroscopy (FTIR) using FTIR-6000 equipment (JASCO, Japan). A shaker (SCI LOGEX SK-O330-pro) was used for adsorption experiments.

### Procedure

#### Production of biochar

After being ground with a size less than 1 mm, the coconut husk was dried at 400 °C for 16 h approximately, then slowly pyrolyzed at 600 °C in an oven without oxygen for 2 h. The heating rate was 5–7 °C/min under a nitrogen flow rate of 5 mL/min. The biochar production yield was calculated using Eq. (1):

$$H = \frac{m_b}{m_0} \times 100\% \quad (1)$$

where  $m_b$  (g) and  $m_0$  (g) were the weight of biochar produced and the input feedstock, respectively.

#### Biochar characterization

The physicochemical properties of the biochar were determined by the electrical conductivity (EC), the cation exchange capacity (CEC), and the pH point of zero charges ( $\text{pH}_{\text{pzc}}$ ). The EC was determined by the ISO 5725 method, CEC was measured by Vietnam's national standard (TCVN 8568:2010), and the point of zero charge ( $\text{pH}_{\text{pzc}}$ ) was analyzed by titration using 0.1 M KCl solution with a biochar/solution ratio similar to the adsorption experiment.

The organic stock solutions at 1000 mg/L of concentration were prepared from levofloxacin, doxycycline, tartrazine, and RhB in the  $\text{HNO}_3$  0.5 M

solution. The simulated solutions (i.e., synthetic wastewater containing organics) were prepared by diluting the stock solutions with an appropriate concentration containing KCl 0.1 M, and the pH value of solutions was adjusted by HCl or NaOH in experiments for the condition specifically.

#### Adsorption experiment

An amount of 25 mg biochar was added into 25 mL of the simulated solutions in a 100 mL Erlenmeyer flask and shaken at 100 rpm using a shaker. The pH value of the solution was adjusted by adding HCl or NaOH solution. The organic concentration was analyzed by spectrophotometer for levofloxacin [16] (a simple method of UV Spectrum at 293 nm), doxycycline [17] (a simple method of UV spectrum at 268 nm), tartrazine (direct measure method in 0.1 M HCl of solution at 482 nm) and RhB (direct measure method in 0.1 M HCl of solution at 554 nm). The adsorption capacity ( $q$ , mg/g) was calculated using Eq. (2).

$$q_i = \frac{(C_0 - C_i) \times V}{m} \quad (2)$$

$C_0$  and  $C_i$  (mg/L) are the organics' initial concentration and the concentration at equilibrium, respectively.  $V$  (L) is the solution volume and  $m$  (g) is the amount of biochar.

#### Adsorption kinetics

The contact time between the adsorbent and the adsorbate is an important parameter, providing information on the sorption kinetics of the adsorbate. The effect of contact time on the adsorption process was determined by an increase in adsorbate concentration on the biochar surface or a decrease in adsorbate concentration in the solution. These results were described in the pseudo-first-order kinetics, the pseudo-second-order kinetics, and the intraparticle diffusion model [18], which were calculated in Eq. (3–5);

$$\ln(q_e - q_t) = \ln q_e - k_1 t \quad (3)$$

$$\frac{1}{q_t} = \frac{1}{t} \frac{1}{k_2 q_e^2} + \frac{1}{q_e} \quad (4)$$

$$q_t = k_i \cdot t^{0.5} + C \quad (5)$$

where  $q_e$  (mg/g) and  $q_t$  (mg/g) are the adsorption capacity of organics at equilibrium and time  $t$  (min) respectively;  $k_1$  ( $\text{min}^{-1}$ ) and  $k_2$  ( $\text{g mg}^{-1} \text{min}^{-1}$ ) are the

equilibrium constants of pseudo-first-order and pseudo-second-order kinetics, respectively;  $k_i$  is the intraparticle diffusion rate constant ( $\text{g mg}^{-1} \text{min}^{-0.5}$ ).  $C$  is the intercept of the plot, which reflects the boundary layer effect or surface adsorption.

#### Adsorption isotherms

The effect of initial concentration on the adsorption process was determined by a change in adsorption capacity which can be calculated using the Langmuir and Freundlich models (Eq. (6) and (7));

$$\frac{C_e}{q_e} = \frac{1}{K_L \cdot q_{\max}} + \frac{C_e}{q_{\max}} \quad (6)$$

$$\log q_e = \frac{1}{n_F} \log C_e + \log K_F \quad (7)$$

where  $q_e$  (mg/g) and  $C_e$  (mg/L) are the organics' adsorption capacity and concentration at the equilibrium, respectively.  $K_L$  (L/mg) is the Langmuir's constant and  $q_{\max}$  (mg/g) is the maximum adsorption capacity which is calculated from the Langmuir equation.  $n_F$  is Freundlich's constant and  $K_F$  (mg/g) is the adsorption constant of Freundlich equation.

#### Adsorption thermodynamics

The effect of temperature on the adsorption process was determined by a change of adsorption capacity in the initial concentration to calculate thermodynamic parameters which show the feasibility and spontaneity of the adsorption process, consisting of Gibbs free energy ( $\Delta G^0$ ), enthalpy ( $\Delta H^0$ ), and entropy ( $\Delta S^0$ ). The change of these parameters was described in Eq. (8–10);

$$\Delta G^0 = -R \times T \times \ln K_d \quad (8)$$

$$\Delta G^0 = \Delta H^0 - T \times \Delta S^0 \quad (9)$$

$$\ln K_d = -\frac{\Delta G^0}{RT} = -\frac{\Delta H^0}{RT} + \frac{\Delta S^0}{R} \quad (10)$$

where  $T$  is the temperature of the solution (K),  $R$  is the gas constant ( $\approx 8.314 \text{ J/mol K}$ ), and  $K_d$  is the distribution coefficient equal with  $q_e/C_e$ .

## RESULTS AND DISCUSSION

### Biochar Production and Characterization

The moisture and the density of coconut husk feedstock were 11.37% and  $0.08 \text{ g cm}^{-3}$ , respectively. The biochar production yield after the pyrolysis process was

approximately 20%, which is lower than the previous research, which is 36% with the same pyrolysis temperature ( $600 \text{ }^\circ\text{C}$  in 2 h). However, due to the pyrolysis rate and furnace being different, the synthesized biochar had a higher surface area [19]. Their physicochemical properties were analyzed, and the results show that the EC was  $6.84 \text{ mS/cm}$ , CEC was  $14.54 \text{ cmol/kg}$  and the  $\text{pH}_{\text{pzc}}$  was 7.73 (Fig. S2), which is higher than the acidic activated biochar, i.e., 6.25 [20]. This shows that the surface charge of the biochar varies depending on the pyrolysis condition and modification method. The biochar surface and pore characterization were analyzed by SEM images, surface area ( $S_{\text{BET}}$ ), pore volume ( $V_p$ ), and pore diameter ( $d_p$ ). The pore size distribution is shown in the Fig. S1. The SEM image (Fig. 1) shows that the biochar's surface has almost macropores and mesoporous forms in the porous structure, with a size range of 2–10 nm major contribution, the pore size average was 4.91 nm, and their surface area and pore volume was  $664.66 \text{ m}^2/\text{g}$  and  $0.8159 \text{ cm}^3/\text{g}$ , respectively. These high surface areas and porous structures were appropriate for adsorption capacity with organics.

During the conversion of coconut husk into biochar, alkali-earth elements, such as potassium (K) and sodium (Na), possibly nucleate, condense, and coagulate together to form a certain amount of ash on the biochar surface [19]. Surface functional groups and minerals are important features of biochar that act as

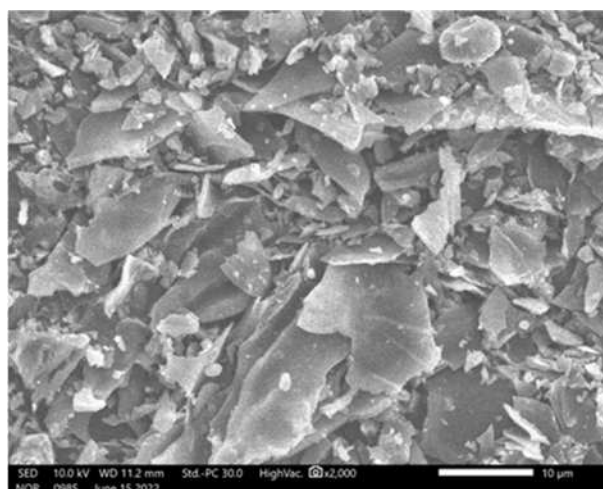


**Fig 1.** SEM image of the biochar

adsorption material. The EDX result revealed the portion of elements in biochar with the main contribution of carbon and oxygen at 90% in total and the other components were Cl, Na, K, Si, Mg, P, Fe, and S elements. All also had an even distribution on biochar surface through mapping results in Fig. 2, which could provide homogeneous active centers for the adsorption process. Maps of elements on biochar surface are also shown in the Fig. S3.

The crystalline structure of biochar based on XRD analysis as shown in Fig. 3(a) that the crystal contained the amorphous form of carbon signed at  $2\theta$ – $30^\circ$  of  $2q$

range, KCl crystals with board peaks of  $2\theta$  at  $28.21^\circ$ ,  $40.53^\circ$ ,  $50.02^\circ$ , and  $66.22^\circ$  (Crystallography Open Database #96-900-3139), and  $\text{SiO}_2$  crystals with board peaks of  $2\theta$  at  $19.58^\circ$ ,  $22.60^\circ$ ,  $23.65^\circ$ ,  $25.54^\circ$ ,  $40.35^\circ$ ,  $50.02^\circ$ ,  $66.22^\circ$  (Crystallography Open Database #46-412-4076). Moreover, the result mapping elements also overlapped the apportioned area of K and Cl, Si, and O elements on the surface.

Carbon, hydrogen and oxygen explain the existence of different surface functional groups on the surface coconut husk biochar produced by pyrolysis and self-sustained carbonization such as carboxyl acid ( $-\text{COOH}$ ),

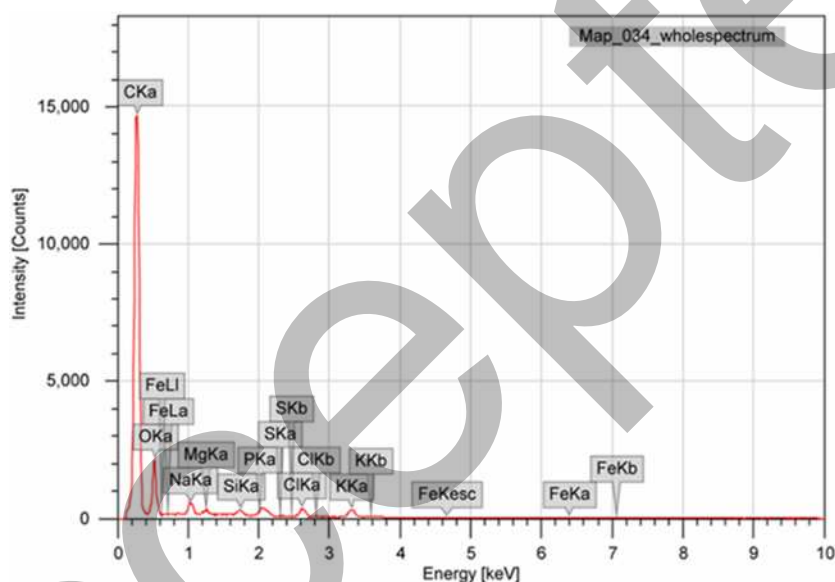


**Fig 2.** EDX spectrum of biochar and its elemental composition

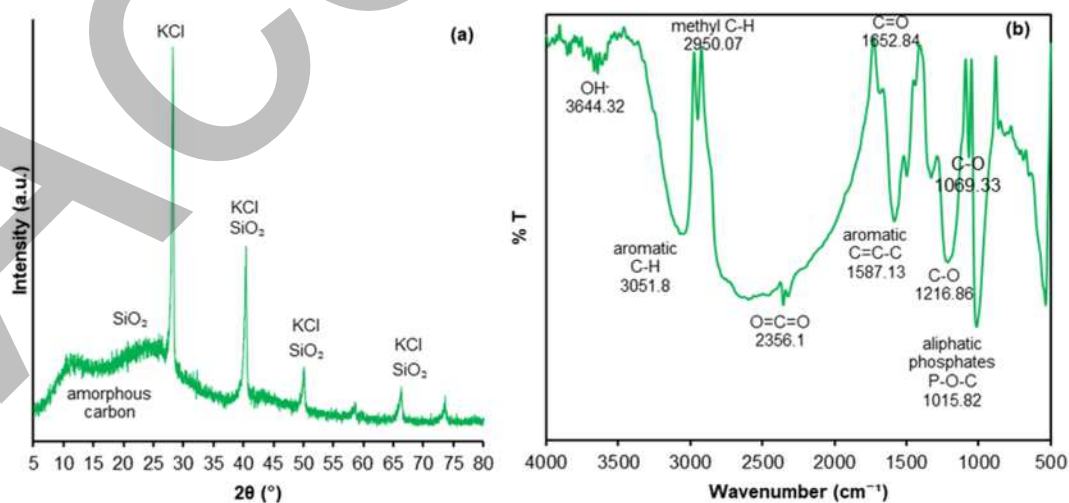


**Fig 3.** (a) XRD and (b) FTIR results of biochar

esters ( $-C=OOR'$ ), aromatic, ketone ( $C=O$ ), iso-cyanide ( $-CH_2-NC$ ), hydroxyl ( $-OH$ ), aryl ethers, quinone, silicon compounds ( $Si-O$ ), alkyl ( $-CH_3$ ), amide ( $O=C-N$ ) and alkyl ether ( $-O-CH_3$ ) group [19]. FTIR result in Fig. 3(b) revealed the chemical composition and structure of biochar. It was the aromatic carbon chain with a stretch peak at  $1587\text{ cm}^{-1}$  ( $1615-2580\text{ cm}^{-1}$ ) of  $C=C-C$  bonds added to  $C-H$  bonds of a peak at  $3051\text{ cm}^{-1}$  [21] and combined functional group of biochar surface including  $-OH$  groups of alcohol, and phenol at peaks in the range of  $3646-3200\text{ cm}^{-1}$ ,  $C-O$  bonds at  $1327\text{ cm}^{-1}$  ( $1390-1310\text{ cm}^{-1}$ , phenol),  $1216$  and  $1069\text{ cm}^{-1}$  ( $1085-1050\text{ cm}^{-1}$ , primary alcohol), carboxylate groups with a peak at  $1552\text{ cm}^{-1}$  (the range of  $1610-1550\text{ cm}^{-1}$ ) added to a peak at  $1331\text{ cm}^{-1}$  (the range of  $1420-1300\text{ cm}^{-1}$ ). The carbon dioxide with the asymmetric stretching peaks at  $2385-2300\text{ cm}^{-1}$  added to the bending bonds at  $668\text{ cm}^{-1}$  were both visible [15,22] as the ability for carbon dioxide capture in the air onto the biochar surface [23].

### Adsorption Mechanism

The mechanism of organic adsorption by coconut husk biochar was proposed, which includes hydrogen bonding, electrostatic interactions, p-p interaction, and

hydrophobic interaction. The adsorption mechanisms could be different depending on the biochar's characteristics, the molecular structure of organic compounds, and environmental conditions like pH solution and temperature. This study was carried out with four different organic compounds to compare the adsorption capacity of different molecular structures in an optimum pH condition. The molecular structures of the four organic compounds and their interaction mechanism with biochar are shown in Fig. 4. The FTIR results show that biochar structure contained  $-OH$ ,  $-COOH$ , and/or amine groups in organics, which created hydrogen bonding with organic adsorbates in the adsorption process, and/or aromatic rings originate for p-p interaction between organics and biochar surface. Additionally, the oppositely charged site on organics and biochar surfaces created electrostatic interactions.

### The Effectiveness of pH solution for The Organic Adsorption onto Biochar

pH can influence the degree of pollutant ionization, the surface properties, and the functional groups of the adsorbent. Therefore, it is the key process factor that can specifically influence the adsorption of

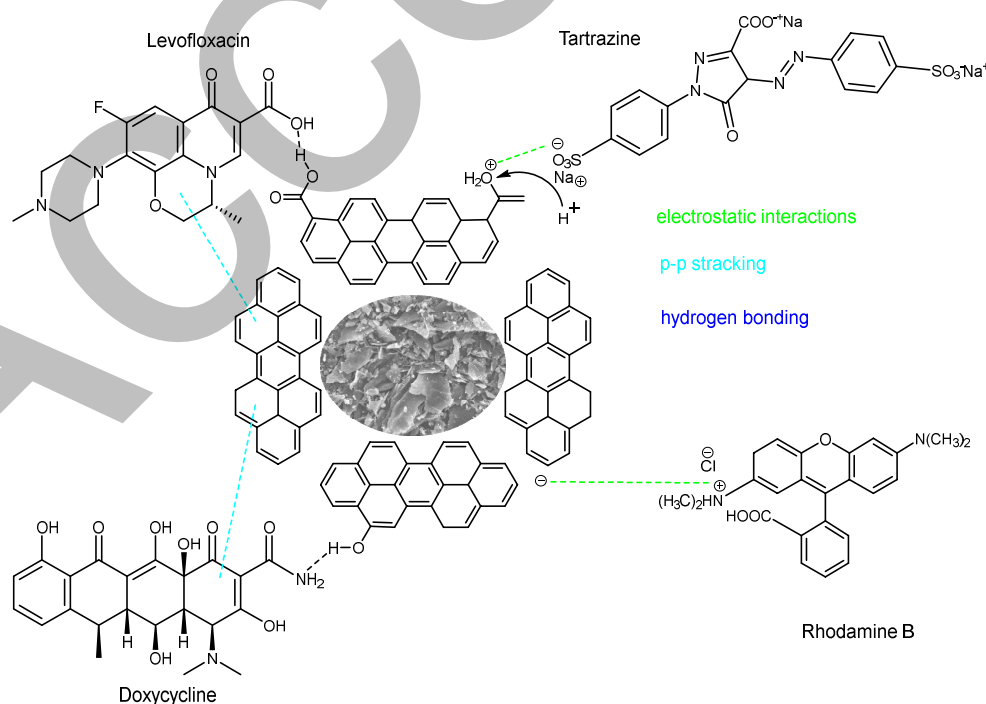


**Fig 4.** The image describes interactions of organics onto the biochar surface

pollutants by adsorbent-adsorbate interactions [24]. An investigation of the pH effect on the adsorption capacity of organics was carried out within the pH range of 2–12. The organic adsorbates introduced in the investigation were Tar, RhB, LEV, and DOX with an initial concentration of 50 mg/L. The results in Fig. 5 revealed that the adsorption capacity of organics onto biochar was higher at lower pH values for Tar, RhB, LEV, and DOX. RhB and DOX compounds were more adsorbed on the biochar than LEV and Tar. The highest adsorption capacity was at pH 2.0 for Tar and RhB, while LEV and DOX were adsorbed higher at pH 5.0.

The organic adsorption onto the biochar surface could be affected by aqueous pH due to the ionization of molecules in the solution, which depended on the biochar characterization and molecules of the organic adsorbates. The distinguished two groups of organics consisted of covalent compounds (i.e., levofloxacin, doxycycline) and ionic compounds (i.e., tartrazine and rhodamine B) that showed different adsorption capabilities.

These interactions are favorable in slightly acidic to neutral pH conditions due to p-p interactions and hydrogen bonds available for the adsorption process as major mechanisms, therefore, all organics could be adsorbed in this pH range (e.g., around pH 5.0 for LEV and DOX). When the aqueous pH turned more acidic (e.g., around pH 2.0), the protonation effects caused an

increase in electrostatic interaction but a decrease in p-p interaction, hydrogen bonding, and hydrophobic interaction simultaneously. Consequently, the adsorption capacity of LEV and DOX dropped slightly, which contrasted with a rise in Tar and RhB adsorption. The RhB cationic organic interaction more than others due to their positive charge in low pH due to strongly attractive with negative charge of biochar surface which would be more available than the pyrolysis at high temperature on that occasion. In the case of Tar, the molecule structure is an anion dye that reached a lower adsorption capacity due to the restriction of electrostatic interaction with the negatively charged surface of biochar. Similar to the previous study [25], the adsorption capacity of RhB is highest at pH 3 on the biochar derived from pine nut shells, while the maximum adsorption capacity of Tar on commercial biochar is at pH 2. The optimum pH conditions are similar in this research, proving that these dyes can adsorb better in more acidic solutions.

For antibiotics, a favorable pH condition gains a weaker acidic solution to neutral due to the charge interaction between molecules and biochar. DOX molecules contain tricarbonylamine, phenolic diketone, and dimethylamine groups; depending on the pH, DOX can be found in cationic ( $\text{pH} < 3.50$ ), zwitterionic ( $3.50 < \text{pH} < 7.07$ ), neutral, and anionic forms ( $\text{pH} > 7.07$ ).

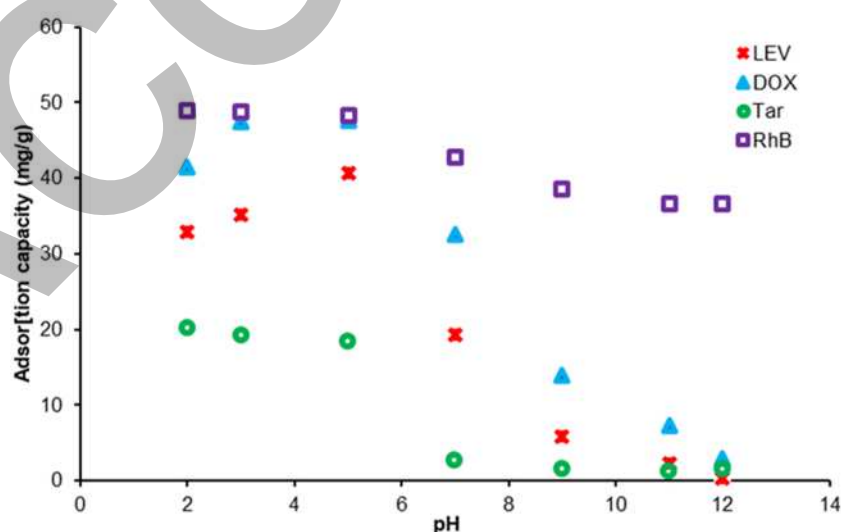


**Fig 5.** The effectiveness of pH condition for adsorption capacity of organics onto the biochar (25 mL solution contained 50 mg/L organics with 25 mg biochar)

Adsorption of DOX by iron-loaded sludge biochar and rice straw biochar in previous studies [26-27] showed that the adsorption maximum was at pH 6 as a result of the abundant neutral particles that cause powerful p-p interactions.

LEV was associated with the prominent cation phase ( $\text{pH} < 6.02$ ), zwitterion phase ( $6.02 < \text{pH} < 8.15$ ), and anion species ( $\text{pH} > 8.5$ ) [27]. LEV adsorption by the synthesized biochar in this study is optimum at pH 5 in a cation phase, which is comparable to previous studies on Fe-biochar and raw biochar (RBC), with the highest adsorption at pH 5.8. Meanwhile, alumina-doped coconut coir charcoal adsorbed LEV at high optimum pH 7 [28-29].

#### Adsorption Kinetics

The contact time significantly affects adsorption

processes and the kinetics of adsorption. Most adsorption processes are completed at longer contact times until equilibrium is reached where no significant change is observed [24]. The dependence of adsorption capacity on contact time at the auspicious pH value was studied. Adsorption kinetics of biochar was studied for LEV, DOX, Tar, and RhB at a concentration of 50 ppm. The results in Fig. 6 showed that the adsorption process reached the equilibrium at around 3 h for the RhB, and almost 1 h for DO, LEV, and Tar.

The kinetic parameters are summarized in Table 1, showing that the pseudo-first-order model was suitable, especially for LEV and RhB, while the pseudo-second-order was suitable for DOX and Tar adsorption. The models' constants were calculated in the same table. The equilibrium contents ( $k_1$  and  $k_2$ ) reflected the adsorption's process speed. In this case, the  $k_1$  of LEV is

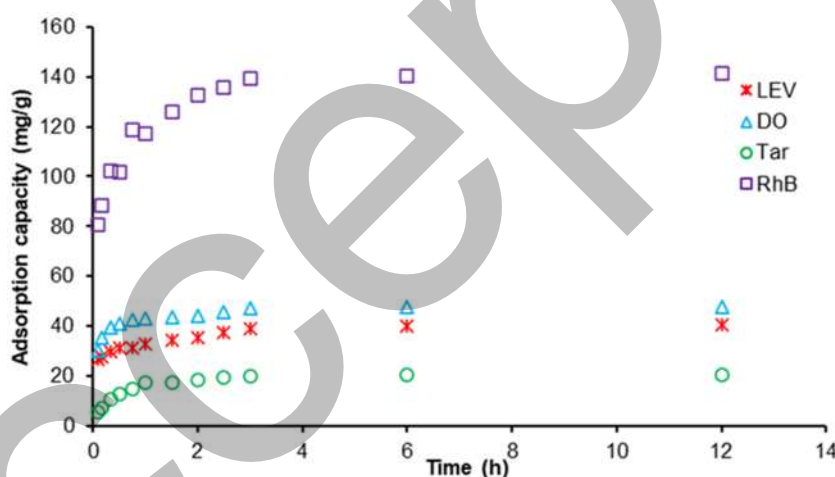


**Fig 6.** Effectiveness of contact time of organics onto biochar (25 mL solution contained 50 mg/L of LEV, DOX, TAR, or 150mg/L of RhB with 25 mg biochar)

**Table 1.** Kinetics' parameters in the adsorption of organics onto biochar

Organics		LEV	DOX	Tar	RhB				
Pseudo-first-order	$R^2$	0.9771	0.9065	0.8534	0.8997				
	$k_1$	0.0098	0.0142	0.0135	0.0117				
	$q_e$ (cal)	14.079	12.225	10.573	45.564				
Pseudo-second-order	$R^2$	0.6999	0.9640	0.9772	0.8476				
	$k_2$	0.0122	0.0132	0.0034	0.0021				
	$q_e$ (cal)	36.101	35.872	19.960	131.58				
Intraparticle diffusion	Phase	1	2	1	2	1	2	1	2
	$R^2$	0.9584	0.7242	0.9242	0.7135	0.9985	0.6333	0.9510	0.6491
	$k_i$	1.0712	0.3398	2.7070	0.2702	2.1523	0.1659	5.8629	0.4577
	C	24.452	32.575	25.783	41.608	0.5685	16.619	71.651	130.41

$0.0098 < k_1$  of RhB  $0.0117$ ; and  $k_2$  of DOX at  $0.0132 > 0.034$  of Tar.

The intraparticle diffusion model describes the adsorption of a solute onto the biochar surface in two phases: external mass transfer and intraparticle diffusion. The first phase corresponded to the boundary layer diffusion, and the second phase was related to the pore diffusion. The first phase reached the linear coefficients in the constraint of over 0.9. The data to be calculated in Table 2 shows the  $k_i$  of phase 1  $>$  phase 2 in all organics. The first phase was faster than the second one, contributing mainly to the total. C values in phase 1 reflect the concentration to be adsorption immediately.

### Adsorption Isotherms

The study of adsorption isotherms was carried out with different initial concentrations from 50 to 100 mg/L for LEV, DOX, Tar, and from 100 to 200 mg/L for RhB to describe the adsorption properties by Langmuir and Freundlich isotherms. The experiment was conducted using a 25 mL solution containing initial organic concentrations mixed with 25 mg Biochar. These results

were shown in Fig. 7, showing an adsorption capacity constant with LEV, DOX, and Tar, which were contrasted with RhB by a significant increase.

The calculated Langmuir's and Freundlich's constants were summarized in Table 3. The linear coefficient of Langmuir isotherm demonstrated the adsorption of organics onto the biochar with  $R^2 > 0.98$  for all organics, proving that the organic molecules were covered in the biochar surface with a monolayer. The Langmuir adsorption has been assumed to occur at specific binding sites that are localized on the surface of the adsorbent, all adsorption sites on the surface of the adsorbent are identical, and there is no interaction between the adsorbed molecules on the adsorbent surface [30]. The maximum adsorption capacity was calculated with  $172.4138 \text{ mgRhB/g} > 48.3092 \text{ mgDOX/g} > 42.3729 \text{ mgLEV/g} > 21.3675 \text{ mgTAR/g}$ . The Freundlich constants were calculated at a value of  $n_f > 1$ , which indicated a multilayer adsorption mechanism. However, this multilayer adsorption was not observed and was heterogeneous with LEV, DOX, and TAR, through lower linear coefficients ( $R^2$ ). On the contrary, the linear

**Table 2.** Parameters of Langmuir and Freundlich isotherms

Organics		LEV	DOX	Tar	RhB
Langmuir model	$q_{\max}$	42.3729	48.3092	21.3675	172.4138
	$K_L$	0.2728	0.5671	0.5081	0.4833
	$R^2$	0.9818	0.9988	0.9985	0.9994
Freundlich model	$n_f$	17.8253	36.2319	32.7869	5.2994
	$K_F$	31.2464	41.2098	18.2390	86.9561
	$R^2$	0.2249	0.3697	0.5959	0.8257

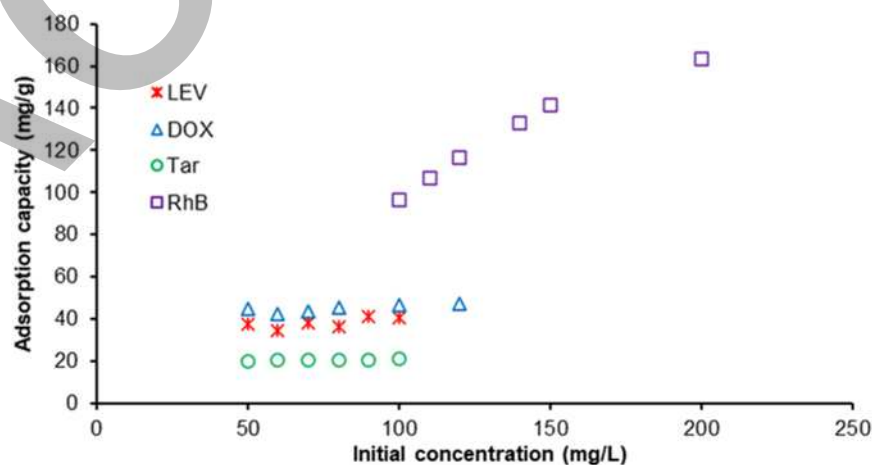


**Fig 7.** Effectiveness of initial concentration for adsorption capacity

coefficient of RhB reached a better value at 0.8257. This was also illustrated in Fig. 5, which shows a significant increase in RhB adsorption capacity corresponding to an increase in initial concentration. The linear plots of adsorption kinetic and adsorption isotherm of the organics onto coconut biochar are shown in Fig. S4.

### Adsorption Thermodynamics

Thermodynamics of the organics adsorption by the coconut husk biochar were studied by the change of adsorption capacity corresponding with the temperature at 28, 40, and 50 °C. The experiment was carried out with 25 mL solutions containing 100 mgLEV/L, 150 mgDOX/L, 50 mgTar/L, and 200 mgRhB/L separately mixed with 25 mg biochar. In Fig. 8, the adsorption capacity of LEV, DOX, and Tar was not changed when the temperature increased, whereas an increase of RhB was observed.

The thermodynamic parameters, which revealed

adsorption properties, were calculated in Table 3. The negative  $\Delta G^0$  value indicated that the adsorption of RhB was spontaneous, compared with non-spontaneous adsorption of LEV, DOX, and Tar due to positive  $\Delta G^0$ . The negative value of  $\Delta G^0$  in RhB adsorption a was dropped when temperature increased, showing that the adsorption of biochar toward RhB was more favorable at higher temperatures.  $\Delta H^0$  indicated the bonding energy of organics onto the biochar surface, in which negative or positive values reflected the endothermic or exothermic process, respectively. That could be a bond breaking and a water molecule displacing adsorption in the total energy changes. In this study, the enthalpy in the range of  $-20$  to  $+20$  kJ/mol implied that the main adsorption mechanism was physical adsorption (e.g., LEV, DOX, Tar), while RhB adsorption is more to be chemisorption with  $\Delta H^0 = 70$  kJ/mol.  $\Delta S^0$  revealed the degree of order or disorder of the system during the

**Table 3.** Thermodynamic parameter of adsorption study

Organics	T (K)	$\ln K_d$	$\Delta G^0$ (kJ/mol)	$\Delta H^0$ (kJ/mol)	$\Delta S^0$ (J/mol K)
LEV	301	-0.6818	18.8334	-4.1595	-19.2070
	313	-0.6344	16.8516		
	323	-0.8048	20.7152		
DOX	301	-1.2139	33.5281	12.7395	31.9773
	313	-1.1195	29.7353		
	323	-0.8538	22.0925		
Tar	301	-0.4249	11.7376	3.1178	7.8948
	313	-0.3495	9.2847		
	323	-0.3425	8.8162		
RhB	301	1.4880	-41.1014	70.0629	245.9364

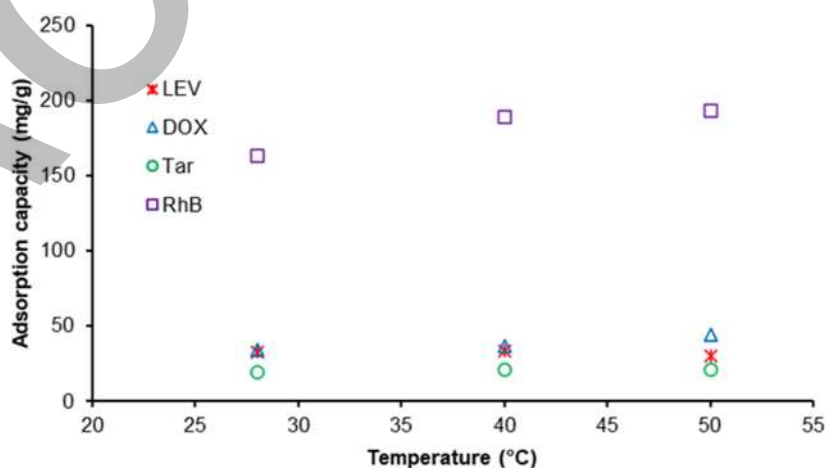


**Fig 8.** Effective of temperature on adsorption capacity of organics

**Table 4.** Adsorption capacity of organics by different biochars

Adsorbent	Biochar feedstock	Surface area (m <sup>2</sup> /g)	Max adsorption capacity (mg/g)	Ref.
Rhodamine B	Coconut husk	664.66	172.41	This study
	coconut shell (Fe-N co-modified)	972.90	12.41	[31]
	Calophyllum inophyllum seed char	155.40	169.50	[32]
	shrimp shells	101.00	350.55	[33]
Levofloxacin	Coconut husk	664.66	42.37	This study
	Coffee bean waste		110.70	[34]
Doxycycline	Coconut husk	664.66	48.31	This study
	Sludge	82.78	128.98	[26]
	Banana peel	710.241	121.95	[35]
Tartrazine	Coconut husk	664.66	21.37	This study
	Commercial biochar	67.20	3.28	[8]
	Coconut cellulose		11.89	[7]

adsorption by negative and positive values, respectively. The  $K_d$  was calculated by the ratio between organics concentration in solid (mg/g) and liquid (mg/L) at the equilibrium. The distribution coefficient value at organics compounds (mg/L) and amount of adsorbents (mg) reflected the performance of the adsorption process, whereas  $K_d > 1$  ( $\ln K_d > 0$ ) reveals the adsorbates performance with this contaminant is higher than 50%, and the amount of adsorbates could be adjusted to increase the adsorption target.

The limitations of biochar on its adsorption performance have been overcome by different modification techniques. The modification methods employed exert significant effects on the physicochemical attributes of biochar. Commonly used modification methods include chemical modification such as iron-loaded magnetic adjustment, acid-alkaline modification, as well as metal and nonmetal modification. Following these modifications, the specific surface area, porosity, and surface functional groups of biochar undergo improvements [31]. Biochar modification can be expensive because it often requires tedious procedures and expensive chemical reagents. Table 4 compares the adsorption capacity of the different biochars on the same organics with this study's results. The results show that biochar production without modification in this study could give high surface area and high adsorption capacity, especially for RhB.

## ■ CONCLUSION

This study reports the successful production of biochar from coconut husk, an abundant agro-waste in Vietnam, using slow pyrolysis at 600 °C following sun drying. The materials were characterized by advanced analysis techniques such as SEM, EDX, XRD, FTIR, and BET, showing that it is a low-cost and good adsorbent due to a porous structure, high surface area of 664.66 m<sup>2</sup>/g with different functional groups, and active centers. Adsorption capacity varied for organic compounds with different molecular structures, such as ionic compounds (RhB, Tar) and covalent bonding (DOX, LEV). The results show that the coconut husk biochar has a more favorable adsorption to the cationic compound (RhB) than the covalent compound DOX, LEV, and the anionic compound (Tar) has the lowest adsorption capacity. The optimum adsorption pH is 2 for RhB, Tar, and slightly higher at pH5 for DOX, and LEV. The results demonstrate that different chemical structures of organic matter affect their treatment ability by adsorption materials, and research on surface improvement to increase adsorption activity is necessary for further study. The adsorption of all organic compounds (RhB, DOX, LEV, Tar) on biochar is suitable to the Langmuir isotherm model, corresponding to macropores and mesopores in the major surface structure. Adsorption kinetics and isotherm studies confirmed the chemisorption

mechanism of RhB on the biochar by the high  $\Delta H^0 = 70$  kJ/mol. The multilayer adsorption property of RhB was illustrated by an extreme increase in adsorption capacity corresponding to an upward movement of initial concentration, which was contrasted with LEV, DOX, and Tar. The results show positive application of agro-waste, i.e., coconut husk to produce an effective biochar at a lower cost and efficiently remove organic pollutants in the wastewater.

#### ■ ACKNOWLEDGMENTS

This research is funded by Vietnam National University - Ho Chi Minh City under grant number C2025-20-20. We acknowledge the support of time and facilities from Ho Chi Minh City University of Technology (HCMUT), VNU-HCM, for this study.

#### ■ CONFLICT OF INTEREST

The authors declare that they have no known competing financial interests or personal relationships that could have appeared to influence the work reported in this paper.

#### ■ AUTHOR CONTRIBUTIONS

Vo Cong Minh conducted the experiment and prepared the draft manuscript, Thuy Nguyen Thi processed the data and visualization, Nguyen Nhat Huy supervised and prepared the draft, and Lien Thi Le Nguyen got funding and revised the manuscript. All authors agreed to the final version of this manuscript.

#### ■ REFERENCES

- [1] Guillotin, S., and Delcourt, N., 2022, Studying the impact of persistent organic pollutants exposure on human health by proteomic analysis: A systematic review, *Int. J. Mol. Sci.*, 23 (22), 14271.
- [2] Obi, C.C., Abonyi, M.N., Ohale, P.E., Onu, C.E., Nwabanne, J.T., Igwegbe, C.A., Kamuche, T.T., and Ozofor, I.H., 2024, Adsorption of antibiotics from aqueous media using nanocomposites: Insight into the current status and future perspectives, *Chem. Eng. J.*, 497, 154767.
- [3] Ahmed, M.N., Abdelsamad, A., Wassermann, T., Porse, A., Becker, J., Sommer, M.O.A., Høiby, N., and Oana, C., 2020, The evolutionary trajectories of *P. aeruginosa* in biofilm and planktonic growth modes exposed to ciprofloxacin: beyond selection of antibiotic resistance, *npj Biofilms Microbiomes*, 6 (1), 28.
- [4] Anh, H.Q., Le, T.P.Q., Da Le, N., Lu, X.X., Duong, T.T., Garnier, J., Rochelle-Newall, E., Zhang, S., Oh, N.H., Oeurng, C., Ekkawatpanit, C., Nguyen, T.D., Nguyen, Q.T., Nguyen, T.D., Nguyen, T.N., Tran, T.L., Kunisue, T., Tanoue, R., Takahashi, S., Minh, T.B., Le, H.T., Pham, T.N.M., and Nguyen, T.A.H., 2021, Antibiotics in surface water of East and Southeast Asian countries: A focused review on contamination status, pollution sources, potential risks, and future perspectives, *Sci. Total Environ.*, 764, 142865.
- [5] Russell, J.N., and Yost, C.K., 2021, Alternative, environmentally conscious approaches for removing antibiotics from wastewater treatment systems, *Chemosphere*, 263, 128177.
- [6] Percivalle, N.M., Carofiglio, M., Hernández, S., and Cauda, V., 2024, Ultra-fast photocatalytic degradation of Rhodamine B exploiting oleate-stabilized zinc oxide nanoparticles, *Discover Nano*, 19 (1), 126.
- [7] Fiorito, S., Epifano, F., Palumbo, L., Colavecchio, C., Bastianini, M., Cardellini, F., Spogli, R., and Genovese, S., 2022, Efficient removal of tartrazine from aqueous solutions by solid sorbents, *Sep. Purif. Technol.*, 290, 120910.
- [8] Soran, M.L., Bocşa, M., Pinteá, S., Stegarescu, A., Lung, I., Opriş, O., 2024, Commercially biochar applied for tartrazine removal from aqueous solutions, *Appl. Sci.*, 14 (1), 53.
- [9] Cano, F.J., Reyes-Vallejo, O., Sánchez-Albores, R.M., Sebastian, P.J., Cruz-Salomón, A., Hernández-Cruz, M.C., Montejo-López, W., González Reyes, M., Serrano Ramirez, R.D., and Torres-Ventura, H.H., 2025, Activated biochar from pineapple crown biomass: a high-efficiency adsorbent for organic dye removal, *Sustainability*, 17 (1), 99.
- [10] Zhou, R., Zhang, M., and Shao, S., 2022, Optimization of target biochar for the adsorption of

- target heavy metal ion, *Sci. Rep.*, 12 (1), 13662.
- [11] Ambaye, T.G., Vaccari, M., van Hullebusch, E.D., Amrane, A., and Rtimi, S., 2021, Mechanisms and adsorption capacities of biochar for the removal of organic and inorganic pollutants from industrial wastewater, *Int. J. Environ. Sci. Technol.*, 18 (10), 3273–3294.
- [12] Tomczyk, A., Sokołowska, Z., and Boguta, P., 2020, Biochar physicochemical properties: Pyrolysis temperature and feedstock kind effects, *Rev. Environ. Sci. Bio/Technol.*, 19 (1), 191–215.
- [13] Ahmed, M.B., Zhou, J.L., Ngo, H.H., Johir, M.A.H., Sun, L., Asadullah, M., and Belhaj, D., 2018, Sorption of hydrophobic organic contaminants on functionalized biochar: Protagonist role of  $\pi$ - $\pi$  electron-donor-acceptor interactions and hydrogen bonds, *J. Hazard. Mater.*, 360, 270–278.
- [14] Ndoun, M.C., Elliott, H.A., Preisendanz, H.E., Williams, C.F., Knopf, A., and Watson, J.E., 2021, Adsorption of pharmaceuticals from aqueous solutions using biochar derived from cotton gin waste and guayule bagasse, *Biochar*, 3 (1), 89–104.
- [15] Zeng, Z., Tan, X., Liu, Y., Tian, S., Zeng, G., Jiang, L., Liu, S., Li, J., Liu, N., and Yin, Z., 2018, Comprehensive adsorption studies of doxycycline and ciprofloxacin antibiotics by biochars prepared at different temperatures, *Front. Chem.*, 6, 80.
- [16] Desai, V.N., Afieroho, O.E., Dagunduro, B.O., Okonkwo, T.J., and Ndu, C.C., 2011, A simple UV spectrophotometric method for the determination of levofloxacin in dosage formulations, *Trop. J. Pharm. Res.*, 10 (1), 75–79.
- [17] Ramesh, P.J., Basavaiah, K., Divya, M.R., Rajendraprasad, N., Vinay, K.B., and Revanasiddappa, H.D., 2011, Simple UV and visible spectrophotometric methods for the determination of doxycycline hyclate in pharmaceuticals, *J. Anal. Chem.*, 66 (5), 482–489.
- [18] Abodif, A.M., Meng, L., Sanjrani, M.A., Ahmed, A.S.A., Belvett, N., Wei, Z.Z., and Ning, D., 2020, Mechanisms and models of adsorption: TiO<sub>2</sub>-supported biochar for removal of 3,4-dimethylaniline, *ACS Omega*, 5 (23), 13630–13640.
- [19] Ajien, A., Idris, J., Md Sofwan, N., Husen, R., and Seli, H., 2023, Coconut shell and husk biochar: A review of production and activation technology, economic, financial aspect and application, *Waste Manage. Res.*, 41 (1), 37–51.
- [20] Adu-Poku, D., Saah, S.A., Sakyi, P.O., Bandoh, C.K., Agyei-Tuffour, B., Azanu, D., Oteng-Pepurah, M., Hawawu, I., Azibere, S., and Affram, K.A., 2024, Acid-activated biochar for efficient elimination of amoxicillin from wastewater, *J. Chem.*, 2024 (1), 3648098.
- [21] Nandiyanto, A.B.D., Oktiani, R., and Ragadhita, R., 2019, How to read and interpret FTIR spectroscopy of organic material, *Indones. J. Sci. Technol.*, 4 (1), 97–118.
- [22] Janu, R., Mrlik, V., Ribitsch, D., Hofman, J., Sedláček, P., Bielská, L., and Soja, G., 2021, Biochar surface functional groups as affected by biomass feedstock, biochar composition and pyrolysis temperature, *Carbon Resour. Convers.*, 4, 36–46.
- [23] Schott, J.A., Do-Thanh, C.L., Shan, W., Puskar, N.G., Dai, S. and Mahurin, S.M., 2021, FTIR investigation of the interfacial properties and mechanisms of CO<sub>2</sub> sorption in porous ionic liquids, *Green Chem. Eng.*, 2 (4), 392–401.
- [24] Huang, B., Huang, D., Zheng, Q., Yan, C., Feng, J., Gao, H., Fu, H., and Liao, Y., 2023, Enhanced adsorption capacity of tetracycline on porous graphitic biochar with an ultra-large surface area, *RSC Adv.*, 13 (15), 10397–10407.
- [25] Atalay Eroğlu, H., Kadioğlu, E.N., and Akbal, F., 2024, High-efficiency removal of Rhodamine B using modified biochar from agricultural waste pine nutshell: Investigation of kinetics, isotherms, and artificial neural network modeling, *Biomass Convers. Biorefin.*, s13399-024-06045-8.
- [26] Wei, J., Liu, Y., Li, J., Zhu, Y., Yu, H., and Peng, Y., 2019, Adsorption and co-adsorption of tetracycline and doxycycline by one-step synthesized iron loaded sludge biochar, *Chemosphere*, 236, 124254.
- [27] Yang, D., Li, J., Luo, L., Deng, R., He, Q., and Chen, Y., 2020, Exceptional levofloxacin removal using biochar-derived porous carbon sheets: Mechanisms

- and density-functional-theory calculation, *Chem. Eng. J.*, 387, 124103.
- [28] Limbikai, S.S., Deshpande, N.A., Kulkarni, R.M., Khan, A.A.P., and Khan, A., 2016, Kinetics and adsorption studies on the removal of levofloxacin using coconut coir charcoal impregnated with Al<sub>2</sub>O<sub>3</sub> nanoparticles, *Desalin. Water Treat.*, 57 (50), 23918–23926.
- [29] Yan, B., and Niu, C.H., 2017, Modeling and site energy distribution analysis of levofloxacin sorption by biosorbents, *Chem. Eng. J.*, 307, 631–642.
- [30] Kecili, R., and Hussain, C.M., 2018, “Mechanism of Adsorption on Nanomaterials” in *Nanomaterials in Chromatography*, Elsevier, Amsterdam, Netherlands, 89–115.
- [31] Li, X., Shi, J., and Luo, X., 2022, Enhanced adsorption of rhodamine B from water by Fe-N co-modified biochar: Preparation, performance, mechanism and reusability, *Bioresour. Technol.*, 343, 126103.
- [32] Behera, A.K., Shadangi, K.P., and Sarangi, P.K., 2024, Efficient removal of Rhodamine B dye using biochar as an adsorbent: Study the performance, kinetics, thermodynamics, adsorption isotherms and its reusability, *Chemosphere*, 354, 141702.
- [33] Pompeu, L.D., Druzian, D.M., Oviedo, L.R., Viana, A.R., Mortari, S.R., Pavoski, G., Espinosa, D.C.R., Vizzotto, B.S., Fernandes, L.S., and da Silva, W.L., 2023, Adsorption of rhodamine B dye onto novel biochar: Isotherm, kinetic, thermodynamic study and antibiofilm activity, *Inorg. Chem. Commun.*, 158, 111509.
- [34] Maged, A., Dissanayake, P.D., Yang, X., Pathirannahalage, C., Bhatnagar, A., and Ok, Y.S., 2021, New mechanistic insight into rapid adsorption of pharmaceuticals from water utilizing activated biochar, *Environ. Res.*, 202, 111693.
- [35] Nguyen, V.T., Nguyen, T.B., Vo, T.D.H., Dat, N.D., Vo, T.K.Q., Nguyen, X.C., Dinh, V.C., Le, T.N.C., Duong, T.G.H., Bui, M.H., and Bui, X.T., 2023, Preliminary study of doxycycline adsorption from aqueous solution on alkaline modified biochar derived from banana peel, *Environ. Eng. Res.*, 29 (3), 230196.